

Stop-and-go kinetics in amyloid fibrillation

Jesper Fonslet^{1,2}, Christian Beyschau Andersen^{3,4}, Sandeep Krishna¹, Simone Pigolotti¹, Hisashi Yagi^{5,6}, Yuji Goto^{5,6}, Daniel Otzen⁷, Mogens H. Jensen^{1†} and Jesper Ferkinghoff-Borg^{8‡}

¹*Niels Bohr Institute, Blegdamsvej 17, DK-2100, Copenhagen, Denmark**

²*Herlev Hospital, Klinisk Fysiologisk Afd. Herlev Ringvej 75, DK-2730.*

³*Novo Nordisk A/S, Protein Structure and Biophysics, Novo Nordisk Park, DK-2750 Måløv, Denmark*

⁴*National Research Council, Institute of Biophysics, Via Ugo La Malfa, 153, I-90146 Palermo, Italy*

⁵*Osaka University, Institute for Protein Research, Yamadaoka 3-2, Suita, Osaka 565-0871, Japan*

⁶*CREST, Japan Science and Technology Agency, Saitama, Japan*

⁷*Århus University, Department of Molecular Biology,*

Gustav Wieds Vej 10 C, 8000 Århus C, Denmark and

⁸*DTU-Elektro, Build. 349, Ørstedss Plads, Technical University of Denmark, 2800 Lyngby, Denmark[‡]*

(Dated: October 28, 2018)

Many human diseases are associated with protein aggregation and fibrillation. We present experiments on in vitro glucagon fibrillation using total internal reflection fluorescence microscopy, providing real-time measurements of single-fibril growth. We find that amyloid fibrils grow in an intermittent fashion, with periods of growth followed by long pauses. The observed exponential distributions of stop and growth times support a Markovian model, in which fibrils shift between the two states with specific rates. Remarkably, the probability of being in the growing (stopping) state is very close to 1/4 (3/4) in all experiments, even if the rates vary considerably. This finding suggests the presence of 4 independent conformations of the fibril tip; we discuss this possibility in terms of the existing structural knowledge.

PACS numbers: 87.14.em 87.15.bk 82.39.-k

Protein fibrillation is the process by which misfolded proteins tend to form large linear aggregates [1]. Its importance is related to the role played in many degenerative diseases, such as Parkinson's, Alzheimer's, Huntington and prion diseases [2]. While our knowledge of the structural properties of these fibrils improves at great pace [3, 4, 5], the dynamics of their growth process is still poorly understood. The formation of amyloid fibrils involves at least two steps: the formation of growth centers by primary nucleation, which is often a slow process, followed by elongation through addition of monomers [6]. In many cases, a so-called secondary nucleation mechanism is also involved, whereby new growth centers are formed from existing fibrils [7, 8, 9, 10, 11]. Whereas the process of secondary nucleation is known to entail a number of different mechanisms [11], the primary elongation process has not been elucidated to the same level of detail.

In this letter, we present an experimental and theoretical study of the elongation process of glucagon fibrils. Glucagon is a small peptide hormone consisting of only 29 amino acids produced in the pancreas. It has the opposite effect to that of insulin and therefore increases blood glucose levels when released. As a model system for protein fibrillation, glucagon kinetics has provided insights into the early oligomerization stages of the process [12, 13, 14, 15], the interplay between growth and fibril morphology [16, 17] and amyloid branching [11]. Here, we focus on the properties of the late-stage elongation process.

Experiments were performed on samples of glucagon

monomers in solution. In order to detect the growth a specialized fluorescence microscopy technique was applied, the so-called Total Internal Reflection Fluorescence Microscopy (TIRFM). This technique utilizes total internal reflection to create an evanescent electromagnetic field adjacent to the glass slide, thereby exclusively exciting fluorophores in only a very thin volume. The penetration depth, d , depends in a specific manner on the wavelength and the angle of the incident light, as well as the refractive indices of the media [18]. In the setup, an argon laser was used along with a fused silica slide in contact with water, leading to a penetration depth of $d = 150$ nm. The TIRFM images of the fibrillation process were obtained at initial glucagon concentration of $\rho = 0.25$ mg/ml in aqueous buffer (50 mM glycine HCl pH 2.5) with preformed seeds. Images of the growth are shown in Fig. 1 at three consecutive times $t = 0, 216, 407$ min. (see [11] for details on the experiment).

Because the fibrils grow along the glass slide we are able to track each fibril length as function of time. We monitor 16 independent fibrils for each image frame in the experiment. The time interval, Δt , between frames varies from a minimum value of $\Delta t_{min} = 1$ min. to a maximum value $\Delta t_{max} = 35$ min., with a typical value of $\Delta t = 10$ min.. The total duration of the experiment is $t = 525$ min. The combined results for the 16 fibrils are shown in Fig. 2.

A striking feature of the fibril dynamics is its discrete nature, where long periods of growth are interrupted by extended periods of stasis (stop state). This prompted

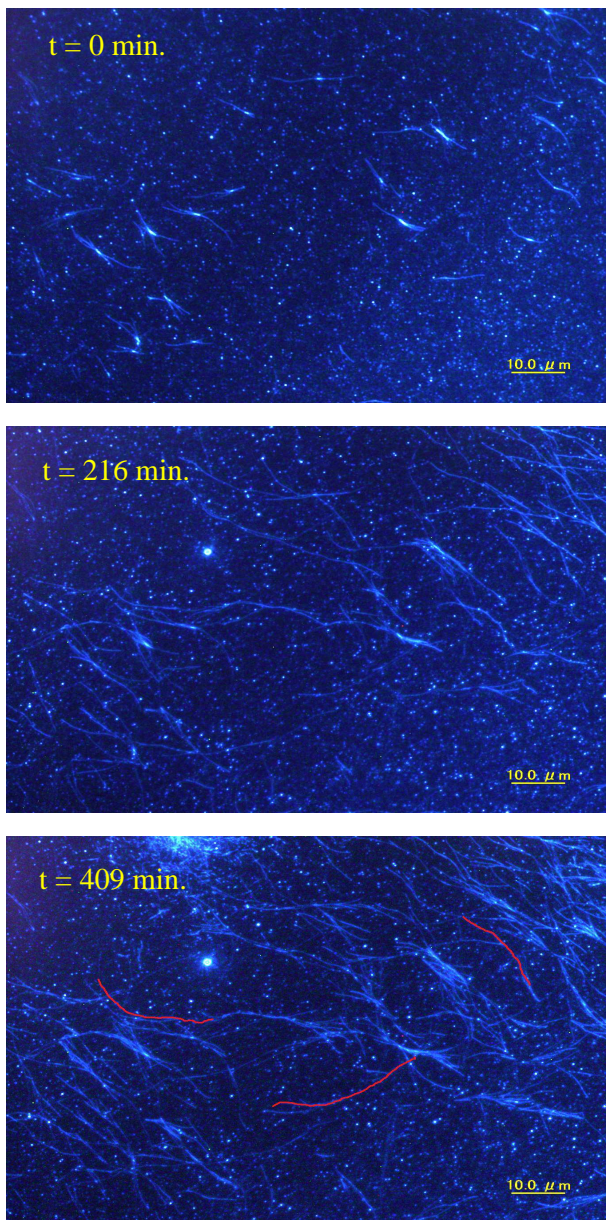


FIG. 1: TIRFM images of glucagon fibril growth with initial glucagon concentration of $\rho = 0.25$ mg/ml in aqueous buffer (50 mM glycine HCl pH 2.5) at three consecutive times after the initiation of the aggregation. Red lines in the last picture mark examples of fibrils which are tracked during the growth process.

us to collect the statistics of time spent in the growth (g) and the stop (s) state, $f_g(t)$ and $f_s(t)$ respectively, for all 16 fibrils. In Fig. 3, these distributions are shown on semi-logarithmic plots. Note that the finite sampling rate implies that actual time spent in given state can only be estimated in terms of upper and lower bounds [19]. The upper estimates are shown by the dashed blue curves and the lower estimates are shown by the full blue curves. As seen in the figure, the difference between

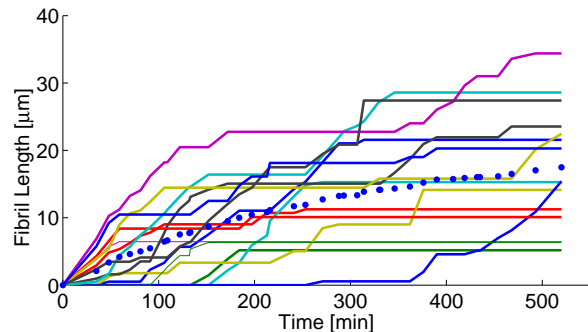


FIG. 2: Length as a function of time for 16 fibrils tracked from the images shown in Fig 1. Note the long plateaus, corresponding to the stop states, followed by shorter (on average) growing periods. The average growth is indicated with a dotted blue line. The sampling time between each image can be seen from the time separation between each point.

the distributions for the upper and lower estimates of both f_g and f_s are marginal. All distributions are very well fitted by exponential functions, $f_g(t) \sim \exp(-k_-t)$ and $f_s(t) \sim \exp(-k_+t)$, as shown by the yellow curves (here, the dashed yellow curve is the fit to the upper estimates and the full yellow curve is the fit of the lower estimates). The fits are of excellent quality over almost two decades, as signified by high R values ($R^2 > 0.98$). The values obtained are $k_+ = 9.0 \cdot 10^{-3} \text{ min}^{-1}$ and $k_- = 2.8 \cdot 10^{-2} \text{ min}^{-1}$. A series of four independent experiments $A - D$ have been performed with the same glucagon monomer concentration (0.25 mg/ml) and pH (2.5) with differences in the seed concentrations ($\sim 20\%$ variation) and data acquisition only. Specifically, the maximal frame length was varied by a factor 3 and the minimum frame length by a factor 18. In all four cases the same analysis and procedure was performed resulting in exponential distributions of similar high quality. The results are summarized in Table I.

The observed stop and go behaviour of fibril dynamics is clearly not associated with the discrete nature of monomer attachment [20]. The simplest model of the process is to assume that the fibril exhibits two internal states: one in which it is allowed to grow, with a rate g and one in which it cannot grow. The intrinsic transition rates between the two states is then identified with the observed transition rates k_+ (stop \rightarrow growth) and k_- (growth \rightarrow stop), see Fig. 4.

The Markovian nature of the model implies, that the time spent in each state is exponentially distributed which is indeed consistent with the results from the data-analysis, Fig.(3), leading to estimates of k_+ and k_- . Denoting the total rate $k = k_+ + k_-$, one can calculate the probability of being in the growing state, $p_+ = k_+/k$ and in the stopped state, $p_- = k_-/k$. Table I presents a summary of the parameters in 4 different experiments. By comparing the four different series, we observe that the

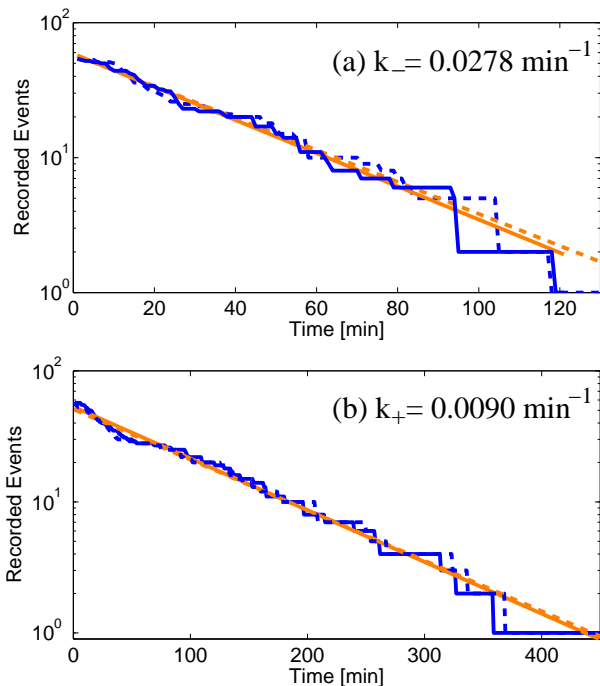


FIG. 3: Growth $f_g(t)$ (a) and stop $f_s(t)$ (b) times distributions on semi-logarithmic scales. Blue lines are data and yellow straight lines are the exponential fit. Both for data and fits, continuous lines are the lower estimates and dashed lines are the upper estimates (see text). All fits are of extremely good quality as indicated by the large R-value, $R^2 > 0.98$.

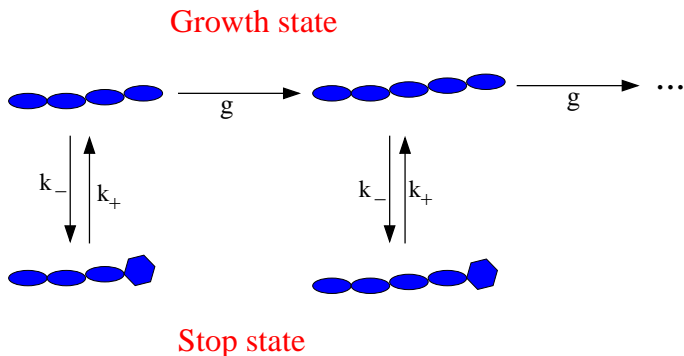


FIG. 4: The simplest two-state model of fibril growth. The fibril is assumed to be in one of two states with intrinsic transition rates of k_+ and k_- . In the growing state, monomer attachment occurs with the rate g .

rates k_+ and k_- vary quite significantly, up to a factor 3. A possible explanation for this could be the variation in sampling frequency (as is indicated in Table I), due to heating of the sample by the laser. Indeed, the dependency of the fibril growth on both the laser intensity as well as the illumination time has been observed under similar experimental conditions for β_2 -microglobulin kinetics [21].

The striking result is that, even though both transition

rates vary among experiments, they combine in such a way that the probabilities of growing and stopping, p_+ and p_- , do not change appreciably in different experiments. In particular, p_+ is always very close to $1/4$ and consequently p_- is very close to $3/4$. Notice that, if the difference between the growing and the stopped state would have been due to an energy gap, one would have expected the population ratio of the two states to be much more sensitive to variations in the individual transition rates, k_{\pm} . Conversely, the constancy of this ratio suggests that the energy difference between the growing and the stopped states to be irrelevant. This ratio could then reflect the presence of three stopped configurations for each growing one, all of them being isoenergetic.

One may wonder whether the observed '1/4-3/4' law is really independent of the monomer concentration, as in the model. Due to experimental limitations, this has not been directly tested. However, the observed average growth rate, g , displays more than a two-fold variation from Exp. A to Exp. D, suggesting notable differences in the local monomer concentration of the growing fibrils. If the state probabilities were sensitive to changes in the concentration, we would have expected a correlation between p_{\pm} and g . We further tried to test the pertinence of the state probabilities by dividing the data sets into two parts, one corresponding to the first half of the experiment and the other to the second half, and measuring p_+ and p_- separately in the two parts. Unfortunately, the statistical noise increased significantly when considering sub-parts of the data series and neither added to nor altered our conclusions.

To conclude, we have presented a stop-go model for glucagon fibril elongation. In fact, similar kinetic behavior has recently been reported for the fibril elongation of $A\beta$ -peptides [22, 23] as well as for α -synuclein [24], although the timescales involved are 1-2 orders of magnitude faster. This suggests that the observed stop-go kinetics reflects the presence of some kind of structural change at the fibril ends, which is not necessarily specific to glucagon. In this picture, the protein properties would affect the barrier height, and thus the timescale of the process, only.

If our hypothesis about the existence of approximately isoenergetic states holds up to scrutiny, it suggests that there may be an additional dimension in the fibrillation energy landscape that cannot easily be identified by conventional techniques. Glucagon is known to adopt a number of different conformations depending on the fibrillation conditions, but these conformations differ considerably in energy and are unlikely to co-exist to an equal extent [25]. Rather, it is possible that we have a number of closely related states with different propagation properties which are separated by high local activation barriers within a relatively flat ground state level. Further experimental studies are required to establish the validity of this suggestion.

Parameters	Exp. A	Exp. B	Exp. C	Exp. D
k_+ [min^{-1}]	0.0090 ± 0.0001	0.0192 ± 0.0004	0.0075 ± 0.0001	0.0059 ± 0.0001
k_- [min^{-1}]	0.0278 ± 0.0005	0.04780 ± 0.00002	0.023 ± 0.002	0.0166 ± 0.0002
p_+	0.244	0.249	0.247	0.260
p_-	0.756	0.751	0.753	0.740
g [nm/min]	135	116	111	56
Tot. time [min]	525	340	630	1030
Max. FL [min]	35	27	24	90
Min. FL [min]	1	3	1	18
Avr. FL [min]	13.7	11.8	20.7	30.9

TABLE I: Estimated kinetic parameters (row 1-5) and parameters for the data acquisition (row 6-9) in 4 different experiments, A-D. FL stands for frame length. All figures of this paper refer to the experiment of the first column, Exp. A. The average growth rate of the fibrils over the total time of each experiment is indicated by g (no appreciable effect of depletion is observed). These values are comparable to the measurements in [11].

This research has been supported by the VILLUM KANN RASMUSSEN Foundation and the Danish National Research Foundations. We are grateful to Christian Rischel and Joachim Mathiesen for discussions at the early stage of this work.

* URL: <http://cmol.nbi.dk>

† Electronic address: mhjensen@nbi.dk, jfb@elektro.dtu.dk

- [1] C.M. Dobson, Nature **426**, 884 (2003).
[2] F. Chiti and C. M. Dobson, Ann. Rev. Biochem. **75**, 333 (2006).
[3] M.R. Sawaya et al., Nature **447**, 453 (2007).
[4] T. P. J. Knowles, J. F. Smith, A. Craig, C. M. Dobson and M. E. Welland, Phys. Rev. Lett. **96**, 238301 (2006).
[5] T. P. J. Knowles, J. F. Smith, G. L. Devil, C. M. Dobson and M. E. Welland, Nanotechnology **18**, 044031 (2007).
[6] S. Chen, F. A. Ferrone and R. Wetzal, Proc. Natl. Acad. Sci. USA. **99**, 11884 (2002).
[7] F. Ferrone, in "Methods in Enzymology", Eds. R. Wetzal, Elsevier Academic Press (San Diego), p. 256 (1999).

- [8] F. Librizzi and C. Rischel. Protein Sci. **14**, 3129 (2005).
[9] S.B. Padrick and A. D. Miranker, Biochemistry. **41** 4694 (2002).
[10] V. Fodera, D. Librizzi, M. Groenning, M. van de Weert and M. Leone, J. Phys. Chem **112**, 3853 (2008).
[11] C. B. Andersen, H. Yagi, M. Manno, V. Martorana, T. Ban, G. Christiansen, D. Otzen, Y. Goto and C. Rischel, Biophys. Jour. **96**(4) 1529 (2009).
[12] A. S. P. Svane, K. Jahn, T. Deva, A. Malmendal, D. Otzen, J. Dittmer and N. C. Nielsen, Biophys. Jour. **95**(1), 366 (2008).
[13] P. A. Christensen, J. S. Pedersen, G. Christensen and D. E. Otzen, FEBS Letters **582**, 1341 (2008).
[14] A.S.P. Svane, K. Jahn, T. Deva, A. Malmendal, D.E. Otzen, J. Dittmer and N.C. Nielsen. Biophys. J. **95**, 366-377 (2008) .
[15] C.L.P. Oliveira, M.A. Behrens, J.S. Pedersen, K. Erbacher, D. Otzen and J.S. Pedersen, J. Mol. Biol. **387**, 147 (2009).
[16] J. S. Pedersen, D. Dikov and D. Otzen, Biochemistry **45** (48), 14503 (2006).
[17] C. B. Andersen, D. Otzen, G. Christiansen and C. Rischel, Biochemistry **46**, 7314 (2007).
[18] T. Wazawa and M. Ueda, in Advances in Biochemical Engineering/Biotechnology, p. 77, Springer, Berlin (2005).
[19] The finite sampling frequency implies that the exact time of a state transition (growth \leftrightarrow stop) can be anywhere in the interval between two observations. Therefore, an upper and lower bound of the time spent in a particular state is simple given by choosing either the 'outer' or the 'inner' observation points.
[20] The monomer attachment rate, r , is approximately given by $r \simeq g\pi R^2/V_{glu} \sim 10^3 \text{ min.}^{-1}$, where $g \sim 100 \text{ nm/min.}$ is the average observed elongation rate (see table I), $R \sim 5 \text{ nm}$ is the fibril radius and $V_{glu} \sim 4 \text{ nm}^3$ is the volume of a fibrillated glucagon peptide. This rate is several orders of magnitude larger than the observed transition rates.
[21] D. Ozawa, H. Yagi, T. Ban, A. Kameda, T. Kawakami, H. Naiki and Y. Goto J. Biol. Chem., **284**, 1009 - 1017 (2009).
[22] M. S. Z. Kellermayer, A. D. Karsai, M. Benke, K. Soo, and B. Penke, Proc. Natl. Acad. Sci. **105**(1), 141 (2008).
[23] Tadato Ban, Masaru Hoshino, Satoshi Takahashi, Daizo Hamada, Kazuhiro Hasegawa, Hironobu Naiki and Yuji Goto. J. Mol. Biol. **344**, 757 (2004).
[24] W. Hoyer, D. Cherny, V. Subramaniam, T.M. Jovin, J. Mol. Biol. **340**, 127 (2004).
[25] J.S. Pedersen and D. Otzen, Protein Science **17**, 2-10 (2008).